The Nucleus ***52****, No. 4 (2015) 151-154*

www.thenucleuspak.org.pk

The Nucleus

ISSN 0029-5698 (Print)

ISSN 2306-6539 (Online)

Structural and Magnetic Studies of $Ni_xCo_{0.8-x}Mn_{0.2}Fe_2O_4$ Nanoparticles Prepared via Co-precipitation Rout

N. Adeela[1,2*], K. Maaz[1*], U. Khan[3], M. Iqbal[2], M. Hussain[1,2], A. Nisar[1], M. Ahmad[1] and S. Karim[1]

[1]*Nanomaterials Research Group, Physics Division, Directorate of Science, PINSTECH, Nilore, Islamabad, Pakistan*

[2]*Centre for High Energy Physics, University of the Punjab, Lahore, Pakistan*

[3]*Institute of Physics, Chinese Academy of Sciences, Beijing 100190, China*

adeela16@gmail.com; maaz@impcas.ac.cn; usman@iphy.ac.cn; skarim73@gmail.com; zahrvi@gmail.com; chempk@gmail.com

ARTICLE INFO

Article history :
Received : 08 September, 2015
Revised : 08 October, 2015
Accepted : 11 December, 2015

Keywords :
Ni doped Co-Mn ferrites,
Structural properties,
Coercivity,
Saturation magnetization

ABSTRACT

Ni substituted Mn-Co ferrite nanoparticles ($Ni_xCo_{0.8-x}Mn_{0.2}Fe_2O_4$), with doping content (x) varying from 0 to 0.1, have been synthesized via co-precipitation route. X-ray diffraction reveals the formation of single phase spinel ferrite structure. Fourier transform infrared spectroscopy exhibits presence of two absorption bands appearing at 500-600 cm^{-1} which are characteristic feature of spinel ferrites. Microstructural analyses were carried out by using scanning electron microscope, transmission electron microscope and energy dispersive X-ray spectroscope which determine the particle size and chemical composition of the synthesized nanoparticles. From TEM results, average particle size was determined to be about 20 nm, which is in good agreement with XRD results. Magnetic results show increase in coercivity and decrease in saturation magnetization with increasing doping concentration.

1. Introduction

Iron oxide based nanostructures have attracted enormous attention since the last two decades due to their relevance to fundamental physics as well as they open up very promising applications. Among these nanostructures spinel ferrites, which are magnetic in nature, play an important role in recent technology. Ferrites have face centered cubic structure with Fd3m space group having a general formula of the form (M^{2+}) $[Fe_2^{3+}]$ O_4 (where M= divalent cation, e.g. Ni, Mn, Zn, Cu) [1]. Magnetic ferrites have stimulated much attention due to their wide range of applications such as high density information storage [2], magnetic fluids [3], catalysts [4-6], recording media [7], microwave devices [8] etc. Among spinel ferrites, cobalt ferrite exhibit remarkable properties like, high permeability, high coercivity, moderate saturation magnetization, large magneto-optic effect, high Curie temperature, high electromagnetic performance along with good chemical stability and mechanical hardness [9].

In cobalt ferrite substitution of Co^{2+} ions with Ni^{2+}, Mn^{2+}, Zn^{2+} etc. allows variation in coercivity and saturation magnetization that can be used in specific applications. Various methods are employed for synthesis of ferrite nanoparticles including sol gel [10], hydrothermal technique [11], ball milling [12], auto-combustion [13], co-precipitation [14], microemulsion [15], solid state reaction [16]. Among these methods co-precipitation has numerous advantages over the others such as easy processing, better control of particle size and size distribution, homogeneous mixing of reactants, high reactivity, and cost effectiveness. In present study, nickel doped cobalt manganese ferrite ($Ni_xCo_{0.8-x}Mn_{0.2}Fe_2O_4$) nanoparticles with average particle size of 20 nm are synthesized by co-precipitation method. Effect of Ni substitution on structural and magnetic properties of Co-Mn ferrites nanoparticles has been studied in detail.

2. Experimental

2.1 Chemicals

Starting materials for the synthesis of nanoparticles were $CoCl_2.6H_2O$, $NiCl_2.6H_2O$, $MnCl_2.4H_2O$ and $FeCl_3$. Sodium hydroxide (NaOH) and oleic acid were used as the precipitating agent and surfactant, respectively. Double distilled deionized water was used as the solvent in order to avoid any impurity in the final product.

2.2 Synthesis of Nanoparticles

$Ni_xCo_{0.8-x}Mn_{0.2}Fe_2O_4$nanoparticles with x=0.0, 0.04, and 0.1 were prepared by co-precipitation method. Starting materials were used in stoichiometric ratio of Ni:Co:Mn:Fe = 1:1:1:2. In the first step, 0.2 molar (M) solutions of cobalt, nickel and manganese chloride were mixed with 0.4M iron chloride solution. Specific amount of oleic acid was added to the mixture while stirring vigorously. 3M NaOH was added drop-wise to the

* Corresponding author

mixture solution under vigorous stirring and was heated at 80°C for one hour. Resultant solution was cooled to room temperature and washed several times with de ionized water and ethanol to remove the impurities. The obtained product was then centrifuged at 4000 rpm for 20 minutes and subsequently dried in the oven for overnight at 100 °C. The dried powder was then grinded to make ultra-fine powder and finally sintered at 600 °C for 6 hours to obtain highly crystalline nanopowder of $Ni_xCo_{0.8-x}Mn_{0.2}Fe_2O_4$.

2.3 Characterization of Nanoparticles

Phase identification and structural analyses of the prepared nanoparticles were carried out by X-ray diffractrometer XRD: RIGAKU-D/MAX-2400) in the range 15°-70° using Cu Kα radiation and wavelength of λ = 0.154056 nm and Fourier transform infrared (FTIR: NICOLET IS-50). Surface morphology and chemical composition were analyzed by scanning electron microscopy (FE-SEM: HITACHI S-4800) and energy dispersive X-ray spectroscopy (EDS). Magnetic measurements were carried out by vibrating sample magnetometer (Microsense EV-9)) with maximum applied field of ± 20 kOe.

3. Results and Discussions

3.1 Structural Analysis

XRD patterns of the nanoparticles with different dopant concentrations are shown in Fig. 1. The patterns show the presence of sharp, intense and well defined peaks confirming the formation of highly crystalline structure of doped spinel ferrites. All peaks were indexed to Fd3m space group with face centered cubic (fcc) cubic symmetry (JCPDS number: 22-1086) [17].

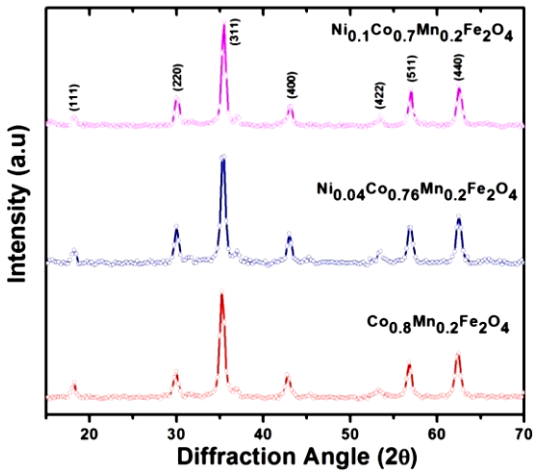

Fig. 1: X-ray diffraction pattern of $Ni_xCo_{0.8-x}Mn_{0.2}Fe_2O_4$($x$=0, 0.04, and 1.0) nanoparticles

Average crystallite sizes were calculated by using Scherrer formula D= 0.9λ/βcosθ and found to be in the range of 19 nm. Where, λ, β and θ are wavelength of radiation used, full width at the half maxima and diffraction angle of respectively. Lattice constants have been computed by using miller indices (hkl) and d spacing using following equation;

$$\frac{1}{d^2} = \left(\frac{h^2 + k^2 + l^2}{a^2}\right)$$

The estimated values of lattice parameter were 8.394, 8.382 and 8.369 Å for doping concentration x=0, 0.04, 0.1 respectively. It has been observed that lattice parameter decrease by increasing Ni concentration. This is because the ionic radius of Ni (0.7 Å) is smaller than the ionic radius of Co (0.83 Å) [17].

3.2 Spectral Analysis

FTIR spectroscopy was used to provide information about the metal cations distribution between the octahedral and tetrahedral lattice sites [18]. FTIR spectra of $Ni_xCo_{0.8-x}Mn_{0.2}Fe_2O_4$ (x= 0.0, 0.04 and 0.1) nano particles in the wavelength range from 3500-400 cm^{-1} are shown in Fig. 2. For spinel ferrites two main absorption bands lie in the range 400-600 cm^{-1} which corresponds to the stretching of octahedral and tetrahedral sites in the crystal structure [18], as shown in inset of Fig. 2. In spinel ferrites the band appearing at 500-600 cm^{-1} is known to be the higher frequency absorption band (υ_1) which attributes to the stretching vibrations of tetrahedral metal complex. This band represents intrinsic vibrations between tetrahedral metal ion and oxygen ion ($M_{Tetrahedral}$-O). While the lower frequency absorption band (υ_2) appearing at 385-450 cm^{-1} represents the stretching vibration of octahedral metal complex with oxygen ion ($M_{Octahedral}$-O). Hence, the presence of these bands strongly suggests the formation of spinel cobalt ferrite nanostructures.

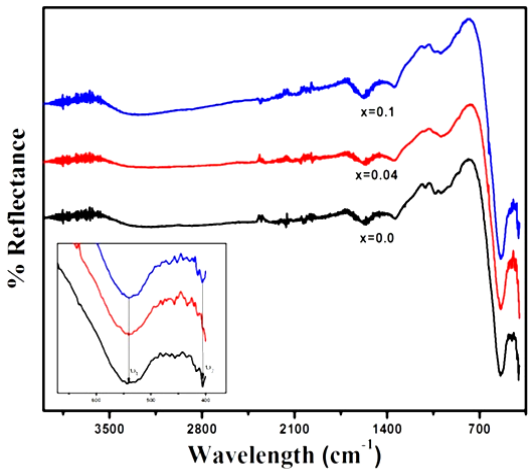

Fig. 2: FTIR spectra of $Ni_xCo_{0.8-x}Mn_{0.2}Fe_2O_4$ (x= 0, 0.4 and 1.0) nanoparticles. Inset: Extended view of frequency bands

3.3 Morphological Analysis

SEM images of Ni substituted cobalt-manganese ferrite nanoparticles with compositions (a) $Co_{0.8}Mn_{0.2}Fe_2O_4$ and (d) $Ni_{0.1}Co_{0.7}Mn_{0.2}Fe_2O_4$ are shown in Fig. 3. The images reveal that the nanoparticles are of uniform sizes with average diameter/particle size lies in the range 25 nm for all compositions. SEM micrographs for x = 0 and 1.0 show similar morphological features that are not affected by the variation in chemical composition. Magnetic interaction among these nanoparticles causes agglomeration of nanoparticles. Chemical composition of synthesized samples was confirmed by energy dispersive X-ray spectroscopy (EDX), shown in the Fig. 3 (b and d). EDX shows the presence of the desired metal cations used during synthesis process.

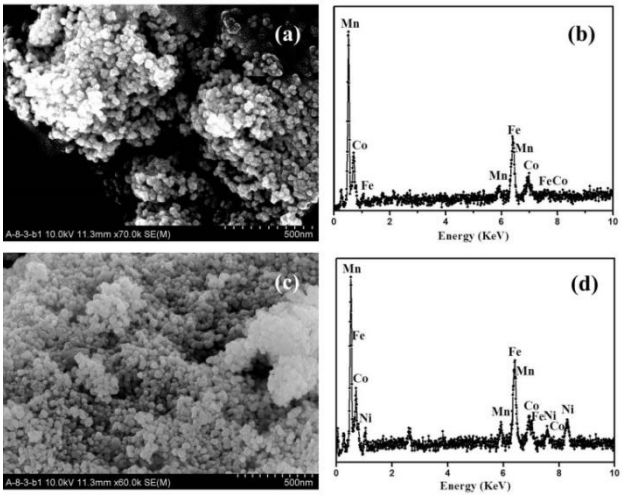

Fig. 3: SEM and EDX observation of (a, b) $Co_{0.8}Mn_{0.2}Fe_2O_4$ nanoparticles, (c,d) $Ni_{0.1}Co_{0.7}Mn_{0.2}Fe_2O_4$ nanoparticles

To get more complete view about particle size and morphology, the transmission electron microscopy of one of the sample was carried out. Fig. 4a shows that synthesized particles have cubic shape and are of uniform size with average particle size of 20 nm which is in good agreement with XRD analysis. It has been observed that

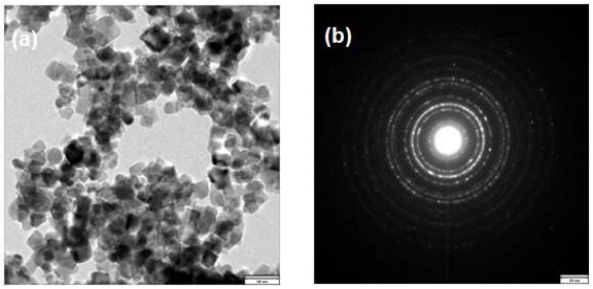

Fig. 4: (a) TEM micrograph of $Ni_{0.1}Co_{0.7}Mn_{0.2}Fe_2O_4$, (b) SAED pattern

some particles tend to agglomerate with each other. This aggregation may arise due to the magnetic interactions among the particles. Fig. 4b represents selected area diffraction pattern (SAED). Here, bright and dark diffraction rings representing different diffraction planes.

3.4 Magnetic Measurements

Magnetic hysteresis loops of the samples are shown in Fig. 5. Inset of figure shows a magnified view of coercivity around the origin. In the figure it is clear that chemical composition affects the magnetic properties of nanoparticles.

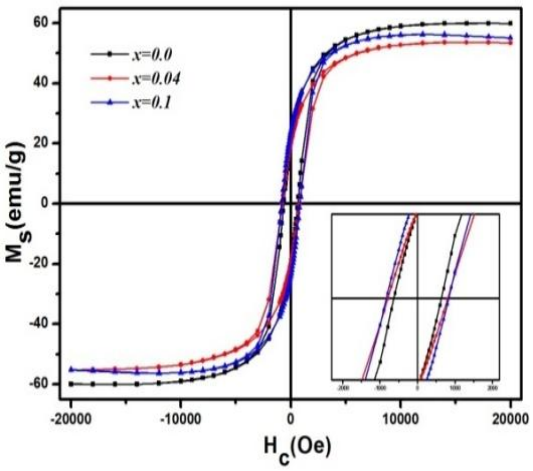

Fig. 5: Hysteresis loops of $Ni_xCo_{0.8-x}Mn_{0.2}Fe_2O_4$ ($0 \leq x \leq 0.1$) nanoparticles with applied field of ±20kOe

It is observed that saturation magnetization decreases with increase in doping concentration. In spinel structure saturation magnetization strongly depends on cationic distribution at the tetrahedral (A) and octahedral (B) lattice sites. The variation of saturation magnetization can be explained on the basis of exchange interactions between both the lattices. Three kinds of exchange interactions occur in a magnetic structure, A-A interaction, B-B interactions and A-B interactions. Apart from chemical composition of the system, magnetic properties also depend on extrinsic parameters, like porosity, density and grain size [19]. In present study, when Ni^{2+} ions ($2\mu_B$) replaces Co^{2+}($3\mu_B$) ions at B sites, then magnetization at B sites decreases, as Ni^{2+} has lower magnetic moment as compared to Co^{2+}. This resultantly decreases the net magnetization (difference of magnetic moments at A and B) with increasing Ni concentration. An increase in saturation magnetization is observed for x= 0.1, which can be attributed to the migration of Fe^{3+} ions from A to B lattice sites on higher doping concentrations [20]. On the other hand, coercivity was found to increase with doping concentration, which is attributed to the strong magneto-crystalline anisotropy of cobalt ferrite and after doping the anisotropy of the system was increased. This increase in coercivity shows that cobalt-manganese ferrite sustains its hard magnetic nature. The coercivity relation with saturation magnetization is expressed by the Brown's relation [21];

$$H_c = \frac{2K_1}{\mu_o M_s}$$

where K_1 is anisotropy constant and μ_o is the permeability of free space. This relation shows that coercivity and saturation magnetization has the inverse relation with each other, which is evident in our samples.

4. Conclusions

In this report we have synthesized Ni doped Co-Mn ferrite nanoparticles with average size of 20 nm. Absorption bands appearing in FTIR spectrum confirms the formation of spinel structure. Magnetic measurements were carried out at room temperature reveals that coercivity increases with increase in doping content, while saturation magnetization shows inverse trend. The synthesized nanoparticles with large coercivity can be used in spintronics.

Acknowledgement

N. Adeela acknowledges University of the Punjab and Pakistan Institute of Nuclear Science and Technology (PINSTECH) for providing research opportunities.

References

[1] L. Kumar and M. Kar, "Effect of La^{3+} substitution on the structural and magnetocrystalline anisotropy of nanocrystalline cobalt ferrite ($CoFe_{2-x}LaxO_4$)", Ceram. Int., vol. 38, pp. 4771-4782, May 2012.

[2] M.N. Ashiq, M.J. Iqbal and I.H. Gul, "Structural, magnetic and dielectric properties of Zr–Cd substituted strontium hexaferrite ($SrFe_{12}O_{19}$) nanoparticles", J. Alloys Compd. vol. 487, pp. 341-345, November 2009.

[3] D.S. Jung and Y.C. Kang, "Effects of precursor types of Fe and Ni components on the properties of $NiFe_2O_4$ powders prepared by spray pyrolysis", J. Magn. Magn. Mater., vol. 321, pp. 619-623, March 2009.

[4] J. Huo and M. Wei, "Characterization and magnetic properties of nanocrystalline nickel ferrite synthesized by hydrothermal method", Mater. Lett., vol. 63, pp. 1183-1184, May 2009.

[5] S. Qaseem, K. Maaz, A. Mumtaz and S.K. Hasanain, "Particle size effect on magnetic and transport properties of $La_{0.7}Ca_{0.3}MnO_3$ nanoparticles", The Nucleus, vol. 47, pp. 137-142, 2010.

[6] N.K. Janjua, M. Mumtaz, A. Yaqub, S. Sabahat and A. Mujtaba, "Electrocatalytic activity of $LiNiPO_4$ and the copper doped analogues towards oxygen reduction", The Nucleus, 51, pp. 109-115, 2014.

[7] Y. Koseoglu, A. Baykal, F. Gozuak and H. Kavas, "Structural and magnetic properties of $Co_xZn_{1-x}Fe_2O_4$ nanocrystals synthesized by microwave method", Polyhedron, vol. 28, pp. 2887-2892, September 2009.

[8] M.H. Sousa, E. Hasmonay, J. Depeyrot, F.A. Tourinho, J.C. Bacri, E. Dubois, R. Perzynski and Y.L. Raikher, "NiFe2O4 nano particles in ferrofluids: Evidence of spin disorder in the surface layer", J. Magn. Magn. Mater., vol. 242, pp. 572-574, April 2002.

[9] A.A. Ati, Z. Othaman and A. Samavati, "Influence of cobalt on structural and magnetic properties of nickel ferrite Nanoparticles", J. Mol. Struct., vol. 1052, pp. 177-182, 2013.

[10] M. Atif, M. Nadeem, R. Grössinger and R.S. Turtelli, "Studies on the magnetic, magnetostrictive and electrical properties of sol–gel synthesized Zn doped nickel ferrite", J. Alloys Compd., vol. 509, pp. 5720-5724, May 2011.

[11] J. Zhang, J. Shi and M. Gong, "Synthesis of magnetic nickel spinel ferrite nanospheres by a reverse emulsion-assisted hydrothermal process", J. Solid State Chem., vol. 182, pp. 2135-2140, August 2009.

[12] S.K. Pradhan, S. Bid, M. Gateshki and V. Petkov, "Microstructure characterization and cation distribution of nanocrystalline magnesium ferrite prepared by ball milling", Mater. Chem. Phys., vol. 93, pp. 224-230, September 2005.

[13] M.H. Yousefi, S. Manouchehri, A. Arab, M. Mozaffari, G.R. Amiri and J. Amighian, "Preparation of cobalt–zinc ferrite ($Co_{0.8}Zn_{0.2}Fe_2O_4$) nanopowder via combustion method and investigation of its magnetic properties", Mater. Res. Bull., vol. 45, pp. 1792-1795, December 2010.

[14] I. Ali, M.U. Islam, M. Ishaque, H.M. Khan, M.N. Ashiq and M.U. Rana, "Structural and magnetic properties of holmium substituted cobalt ferrites synthesized by chemical co-precipitation method", J. Magn. Magn. Mater., vol. 324, pp. 3773-3777, November 2012.

[15] X. Gao, Y. Du, X. Liu, P. Xu and X. Han, "Synthesis and characterization of Co–Sn substituted barium ferrite particles by a reverse microemulsion technique", Mater. Res. Bull., vol. 46, pp. 643- 648, May 2011.

[16] D.-H. Chen and X.-R. He, "Synthesis of nickel ferrite nano particles by sol-gel method", Mater. Res. Bull., vol. 36, pp. 1369-1377, May 2001.

[17] N. Adeela, K. Maaz, U. Khan, S. Karim, A. Nisar, M. Ahmad, G. Ali, X.F. Han, J.L. Duan and J. Liu, "Influence of manganese substitution on structural and magnetic properties of $CoFe_2O_4$ nanoparticles", J. Alloys Compd., vol. 639, pp. 533-540, August 2015.

[18] R.D. Waldron, "Infrared spectra of ferrite", Phys. Rev., vol. 99, pp. 1727–1735, September 1955.

[19] J. Smith and H. P. J. Wijn, "Ferrites", Philips Technical Library, London, 1959.

[20] M.A. Khan, M.J. Rehman, K. Mahmood, I. Ali, M.N. Akhtar, G. Murtaza, I. Shakir and M.F. Warsi, "Impacts of Tb substitution at cobalt site on structural, morphological and magnetic properties of cobalt ferrites synthesized via double sintering method", Ceram. Int., vol. 41, pp. 2286–2290, 2015.

[21] S. E. Shirsath, B. G. Toksha, and K. M. Jadhav, "Structural and magnetic properties of In^{3+} substituted $NiFe_2O_4$", Mater. Chem. Phys. vol. 117, pp. 163-168, September 2009.